Multiphase Materials with Lignin. IV. Blends of Hydroxypropyl Cellulose with Lignin

TIMOTHY G. RIALS* and WOLFGANG G. GLASSER, *Department of Forest Products and Polymer Materials and Interfaces Laboratory, Virginia Polytechnic Institute and State University, Blacksburg, Virginia 24061*

Synopsis

Polymer blends of hydroxypropyl cellulose (HPC) and organosolv lignin (OSL) were prepared by mixing in solutions of both pyridine and dioxane, and casting as films, and by mixing in the melt followed by extrusion. All preparations exhibited partial miscibility as evidenced by a single T_g up to a composition of 40 wt % lignin above which phase separation was detected. Dioxane-cast and injection-molded blends were distinguished from the pyridine-cast materials by a positive T_g deviation from additivity, an approximation which adequately described the latter. This positive deviation in T_g is attributed to the formation of a liquid-crystal mesophase with a resultant reduction of amorphous HPC available for interaction with the lignin component. This explanation is supported by a rapid rise in modulus (~150%) and tensile strength with very low lignin content, and by an associated sharp decline in ultimate elongation. The development of morphological features, as observed by scanning electron microscopy provide further substantiation of this hypothesis.

INTRODUCTION

Two prior publications in this series have dealt with the structure and properties of polymer blends between two commercial thermoplastic polymers, poly(methyl methacrylate) and poly(vinyl alcohol), and a lignin derivative, hydroxypropyl lignin. These have demonstrated that at least partial miscibility is achieved if (a) the solubility parameter of both components approaches a similar value and (b) sufficient polymer–polymer interaction occurs through such forces as hydrogen bonds. A natural extension of this work involves the exploration of polyblend behavior of lignin (and its derivatives) with amorphous and semicrystalline polysaccharides—systems that resemble the biocomposite, wood.

In general, when two polymers are blended together, they may exist either in a completely homogeneous state where their chain segments are mixed at the most intimate level or they may segregate into distinct regions or phases.[1] The ability to predict the morphology of a polymer pair, in terms of the degree of phase separation or miscibility, is largely dependent on the extent of interaction between the two polymers. Although immiscible systems are not

*Current address: Southern Forest Experiment Station, Pineville, LA. Direct all inquiries to the second author.

Journal of Applied Polymer Science, Vol. 37, 2399–2415 (1989)
© 1989 John Wiley & Sons, Inc.
CCC 0021-8995/89/082399-17$04.00

immediately excluded from interest, the production of novel materials with unique thermal, mechanical, or optical properties requires that the polymer pair be miscible. The definition of a miscible system as a single-phase material limits this to mixtures of amorphous polymers.[2,3] Crystallization will necessarily produce an immiscible system since the definition requires that a new crystal structure be formed when the system is truly miscible. Studies on binary systems containing a crystallizable component have recently received considerable attention from practical and theoretical considerations. The best known example involves blends with poly(vinylidene fluoride).[4-6]

Binary blends containing rigid, rodlike chain polymers, such as the aromatic polyamides that exhibit thermotropic liquid crystal (LC) behavior,[7] may provide the basis for unique high modulus, high strength composite materials.[8] Although thermotropic LC polymers have been synonymous with copolyesters, recent results[9] with a polyamide have demonstrated a dramatic increase in both modulus and tensile strength with an increase in the liquid crystal component. Similar results were reported by Joseph et al.[10] from work involving poly(ethylene terephthalate) blends.

The scope of LC polymers is greatly expanded upon consideration of lyotropic systems, which form mesophases above a critical solution concentration. Polymers that have been reported as exhibiting this behavior include polypeptides, polyamides, polyisocyantes,[11] and certain cellulose derivatives.[12] Of the numerous liquid crystal cellulosics, hydroxypropyl cellulose (HPC) has been the model system of choice in the evaluation of parameters influencing mesophase formation and structure.[13-15] Preliminary investigations on oriented HPC films prepared from LC-doped solutions have produced only moderate increases in material strength.[16] Consequently, the utilization of HPC as a component in polymer blends is a concept that has been largely overlooked, despite significant practical and fundamental implications. One particularly intriguing composite system involving HPC is that which resembles the lignocellulosic combination of the wood cell wall. In this biological material, the carbohydrate component is intimately associated with lignin—an aromatic polymer comprised of phenylpropane units.[17] Conventionally described as a 3-dimensionally crosslinked polymer, lignin's biological function is perceived as a structural matrix imparting strength and rigidity to the cell wall. The morphology of this composite has not yet been clearly defined, an aspect that has been emphasized by recent reports indicating that the *in situ* lignin may exist in a more ordered state than was considered in original treatments of the subject.[18] What is clear, however, is that there exists a unique relationship between lignin and the carbohydrate component with which it is associated. It remains to be seen if the distinctive affinity of these two polymers can be established upon combination of the isolated components to form new and useful polymer composites.

Polymer blends from lignin and HPC may be formed in a variety of processing modes. Because of the lyotropic and thermotropic nature of HPC, the influence of solvent and temperature, as well as the degree of association of lignin[19] could dramatically affect overall blend morphology and properties. The evaluation of lignin/HPC blends is therefore to consider the method of preparation. This may be from solution (dioxane or pyridine), or by melt mixing followed by injection molding.

TABLE I
Pertinent Structure and Property Data of Hydroxypropyl Cellulose (HPC) and Organosolv Lignin (OSL)

Component	Total OH (wt %)	Phenolic OH (wt %)	$\langle M_n \rangle$ (g M^{-1})	$\langle M_w \rangle$ (g M^{-1})	ρ (g cm^{-3})	δ [(cal $cm^{-3})^{1/2}$]	T_g (K)	T_m (K)
HPC	12.2	—		100,000[a]	1.17	10.7	298	485
OSL	8.4	6.1	900	3,000	1.24	11.2	385	—

[a]As per information provided by supplier.

EXPERIMENTAL

Sources and Characterization of Components

The hydroxypropyl cellulose (HPC) utilized in the study was provided by Hercules, Inc. (Klucel "L"). The molar substitution, as reported by the manufacturer, was four propylene oxide units per anhydroglucose unit and the nominal molecular weight (M_w) was 100,000 g/mol.

An organosolv (ethanol) lignin (OSL) preparation, isolated from aspen wood, was obtained from the Biological Energy Corp. of Valley Forge, PA. Details of the yield and isolation conditions were not made available. The molecular weight was determined by gel permeation chromatography to be $\langle M_n \rangle = 900$ and $\langle M_w \rangle = 3000$. Pertinent structure and property data of the homopolymers are complied in Table I.

Preparation of Blends

The HPC/OSL blends were prepared by mixing in solution and mixing in the melt. Individual solutions of the components were prepared (~5 wt %) using both dioxane and pyridine. The solutions were then mixed together and stirred for approximately 12 h before they were cast into Teflon molds. The films were kept at ambient conditions for 24 h before being dried under vacuum 80°C for 1 week. The resultant films were stored over P_2O_5 in a vacuum desiccator.

Extruded blends were prepared with a Custom Scientific Instruments Mini-Max injection molder. The extrusion temperature was 170°C and the residence time was no longer than 5 min. The blended material was extruded into a warm, dog-bone mold for testing.

Differential Scanning Calorimetry (DSC)

Thermal properties of blends were determined on a Perkin-Elmer DSC-4 interfaced to the thermal analysis data station. All samples were scanned at a heating and cooling rate of 20°C/min under a purge of dry nitrogen. The glass transition temperature (T_g) was defined as one-half the incremental change in heat capacity at the transition. The melting temperature at which the last crystal melt was observed while crystallization temperatures were taken as the peak maximum temperature.

Dynamic Mechanical Thermal Analysis (DMTA)

Dynamic mechanical properties were determined with the Polymer Laboratories DMTA interfaced to a Hewlett-Packard 9816 microcomputer. Samples were tested using a single cantilever beam geometry and a frequency of 10 Hz. A heating rate of 4°C/min was employed for all samples.

Mechanical Properties

Uniaxial stress-strain properties were determined in tension with a standard Instron testing machine. A crosshead speed of 1 mm/min was employed on samples that were cut with a die in a dog-bone shape (solvent cast films); or, in the case of extruded samples, a dog-bone mold was used. Tensile properties were calculated on the basis of initial dimensions (gauge length = 10 mm, film area $\approx$ 0.71 mm^2 and extruded sample area $\approx$ 4.2 mm^2).

Wide Angle X-Ray Scattering (WAXS)

Wide angle X-ray diffraction patterns of the blended materials and their component polymers were obtained in the reflection mode using a Phillips diffractometer with a CuKα source. Sample thickness was approximately 0.01 in.

Scanning Electron Microscopy (SEM)

Scanning electron micrographs were taken on an Amray Model AMR-900 microscope. Surfaces were prepared by freezing in liquid nitrogen and fracturing. The fracture surface was sputter-coated with carbon and a gold-palladium alloy.

RESULTS AND DISCUSSION

Thermal Properties

Glass Transition (T_g) Behavior. The state of miscibility of a polymer pair is conveniently assessed by evaluating T_g.[3] Phase-separated blends exhibit the T_g of the two individual homopolymers while a unique, intermediate value is typically observed in miscible materials. Figure 1 shows a series of thermograms of varying compositions for the HPC/OSL blends prepared by injection molding. A single T_g is observed up to a lignin content of 55% where two glass transitions are detected at 70 and about 130°C. The higher T_g in the 55–85% lignin blends is slightly above that of the pure lignin component (i.e., 115°C). At lower lignin contents, T_g rises and displays noticeably increased sharpness and intensity as the lignin content is increased to 40 wt %. This observation may be interpreted with the depression of a transition at 70–110°, which has been related in earlier work to a residual LC mesophase found in HPC. Apparently, as the lignin content of the blend rises, this transition is shifted to lower temperature and effectively masks the amorphous phase T_g. At 40% lignin content, the mesophase structure is disrupted to the point that the conventional step increase associated with a glassy state transition becomes clearer.

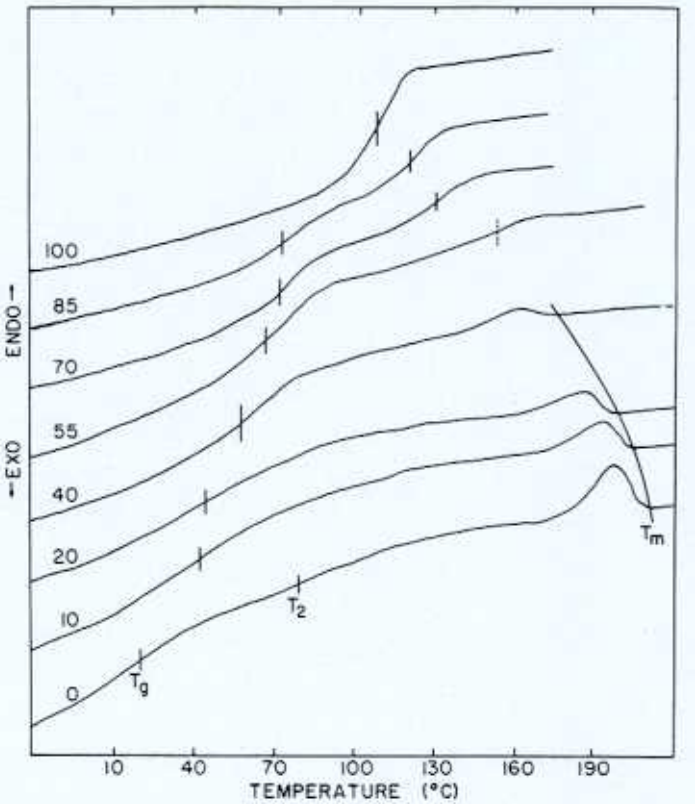

Fig. 1. The effect of blend composition on thermal properties of extruded preparations. (The numbers associated with each curve give the weight of lignin in the material.)

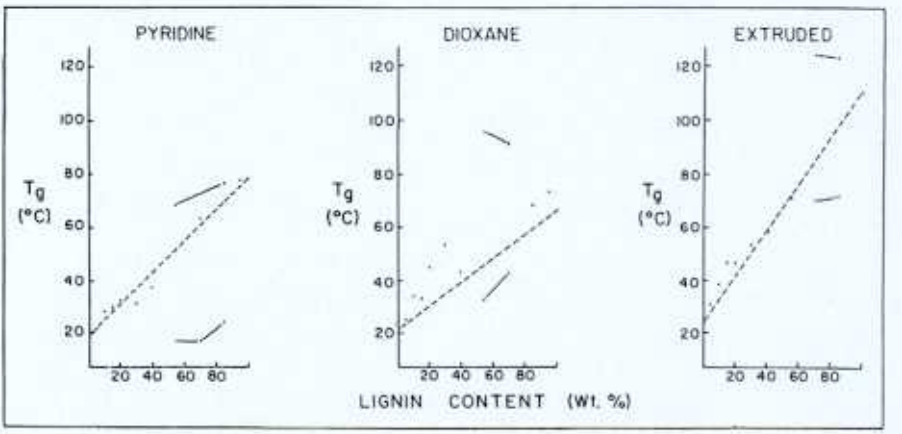

Fig. 2. The variation in glass transition temperature (T_g) with blend composition for materials prepared by solvent casting from (A) pyridine and (B) dioxane, and (C) melt extrusion.

Figure 2 shows a comparison between the blends prepared by solvent casting and injection molding. All of these systems display a single T_g when the lignin content is below 50%. In the case of materials blended in pyridine, the T_g follows the rule of mixtures. By contrast, the material blended in dioxane and in the melt show a significant positive deviation from additivity.† Although this type of deviation has served as an indicator of hydrogen bonding in a number of binary polymer blends,[20] it can also be accounted for by a somewhat lower amorphous fraction than was estimated for the HPC homopolymer. This would result in a higher lignin fraction in the miscible portion of the blend and, thus, a higher T_g. Although less likely, if some interaction existed between lignin and the mesophase component, the increased organization could result in a T_g above that expected.

The transition temperatures of the separated phases are shown in Figure 2 to be dependent on the mode of blend preparation. The dioxane-cast and extruded materials exhibit T_g's at higher temperatures than the corresponding pure components. This may indicate the preferential inclusion of high molecular weight species in the resulting lignin-rich domains, an explanation consistent with the conclusion that the HPC/OSL blend represents a partially miscible system.

Polymer relaxation processes can generally be detected by dynamic mechanical analysis (DMTA) with greater sensitivity when compared to DSC. Results on the injection molded samples are shown in Figure 3. The tan δ spectrum of pure HPC reveals two primary relaxations, one at 30°C (T_1) and one at 85°C (T_2). These have been previously assigned to the amorphous component T_g and a more highly organized, liquid crystal mesophase, respectively.[21] The T_2 relaxation corresponds to the less distinct high temperature transition observed by DSC (see Fig. 1). The effect of lignin content is manifested by an increased intensity of the T_2 peak, apparently at the expense of the amorphous component's relaxation. This implies a preferential association of lignin with the liquid crystal mesophase to the exclusion of the amorphous phase of the HPC and is consistent with earlier observations. Although unusual, this interpretation cannot be ruled out and receives added evidence from literature reports on: (a) monolayer film studies that have indicated that lignin is essentially discotic, or planar, in character[22]; (b) solution association phenomena in lignin[19]; and (c) *in situ* orientation of lignin in whole wood.[18] Collectively, this evidence suggests that lignin actually exists in a more ordered state than has been traditionally recognized. With the evidence suggesting some type of ordered morphology in lignin, the possibility of mesophase enhancement cannot be dismissed as readily. Further evidence of the lignin's influence on supermolecular structure can be found in the increased intensity and sharpness of the tan δ peak and storage modulus (E′) behavior of the blends with lignin contents between 20 and 40%. No decrease

†It should be noted that this deviation may not be as great as it appears in the dioxane cast blends as the T_g of the pure lignin (cast from dioxane) was inexplicably found to be about 40° lower than that of the extruded and original lignin sample; a 25° depression was observed when the lignin was cast from pyridine. There remains, however, an obvious distinction between the pyridine-cast blends and the other preparations in that a consistently lower T_g was observed than was expected.

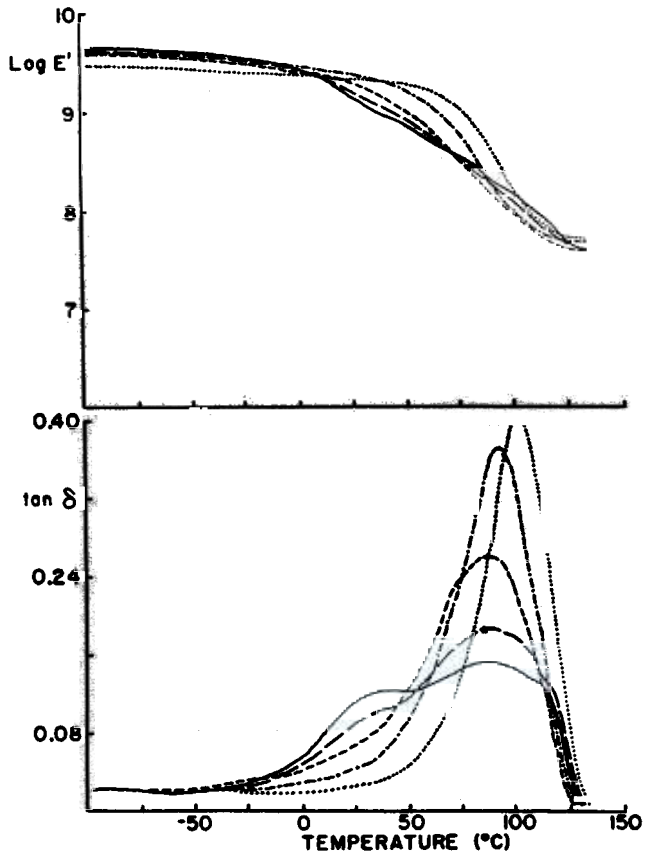

Fig. 3. The influence of lignin content on the dynamic mechanical properties (tan δ and log E') of extruded HPC/OSL blends at the following compositions: (——) pure HPC; (– –) 5%; (- - - -) 20%; (– · – ·) 40%; (· · ·) 55%.

TABLE II
Summary of Transition Temperatures (T_1 and T_2) from Dynamic Mechanical Thermal Analysis of HPC/OSL Blends Prepared by Different Methods

Lignin content (wt %)	Solution-cast				Injection-molded	
	Pyridine		Dioxane			
	T_1[a] (K)	T_2 (K)	T_1 (K)	T_2 (K)	T_1 (K)	T_2 (K)
0	299		298	342	310	362
5	296		298	343	313	365 (67)
10	300		300	351	—[d]	359 (66)
15	296		302	353	—	360 (56)
20	309		307	356	—	360 (56)
30	310		+	+	—	364 (49)
40	318		+	+	—	366 (40)
55	+[b]		+	+	—	373 (38)
70	+		+	+	—	379 (42)

[a] T_1 peaks appeared as shoulders above 10% lignin content in both pyridine- and dioxane-cast blends.

[b] Indicates transition was not clearly defined.

[c] Values in parentheses represent peak widths at half-maximum.

[d] No peak was observed.

[e] Materials were too brittle for analysis.

of log E' is observed for the 40% blend until about 45°C, while the lower lignin content blends exhibit a loss in modulus beginning at about 0°C. This behavior is in agreement with DSC results, and it is consistent with the supposition of a modified phase morphology.

The transition temperatures determined by DMTA are summarized in Table II. The results indicate the presence of at least a shoulder for the T_1 transition (< 40% lignin contents) in the solvent-cast blends which exhibits a slight composition dependence. This indicates that the increased intensity of the T_2 peak may result from the convolution of the two relaxation processes, rather than an increased mesophase content. While it cannot be definitively concluded that lignin preferentially interacts with either the amorphous phase or the LC mesophase of HPC, it is apparent that partial miscibility is achieved up to a lignin content of 40%.

Melt Behavior. A summary of melting data for the HPC/OSL blends is presented in Table III. Generally, a consistent decrease in the magnitude of all parameters with increasing lignin content is observed. At the highest lignin level where crystallinity could be accurately measured, the pyridine- and injection-molded preparations show a T_m depression of about 40°C. The dioxane-cast blends maintained a consistently higher T_m. Heat of fusion (ΔH_m), however, indicates that both the dioxane- and injection-molded blends are essentially identical, which is consistent with the observed behavior in T_g. The pyridine-cast blends showed slightly higher ΔH_m values until the blend composition reached 40% lignin. Interestingly, whereas the presence of crystallinity vanished at ca. 40% lignin, there remains a substantial crystallization window ($T_m - T_g$), of about 120°C for the injection-molded materials at this composition. Typically, crystallinity would not be expected to be lost until this window is much smaller,[23] although this may simply be in response to the relatively low level of crystallinity developed in HPC.

The heat of melting of a perfectly crystalline HPC (ΔH_u) has been estimated by Samuels[24] to be −6.44 cal/g and allows the degree of crystallinity to be computed. The results for the HPC/OSL blends are shown in Figure 4. All preparations exhibit a loss of crystallinity with lignin content rising, as is expected. The blends experience a more rapid loss of crystallinity than that predicted simply by considering the reduced volume fraction of the crystallizing component, especially those prepared from dioxane- and injection-molding. Pyridine-cast blends retain more crystallinity, and this is consistent with differences in T_g behavior. The reduction of the crystalline phase is, however, not synonymous with added amorphous volume fraction which would be reflected in a more pronounced T_g. The observed failure to affect the intensity of the T_g at lower lignin contents may again be explained by the formation of liquid crystal mesophases which have been reported both in dioxane[25] and at the extrusion temperature[26] of 170°C. The extent of interaction between the lignin component and HPC mesophase remains ambiguous at this point.

The evaluation of crystallinity by WAXS is illustrated in Figure 5. Pure HPC shows two peaks at $2\Theta = 8°$ and at $2\Theta = 20.3°$ which have been assigned previously[24] to the 100 equatorial reflection and a slightly oriented amorphous component, respectively. The lignin component is characterized by a broad, amorphous peak centered at about $2\Theta = 21.7°$. A small peak is also found at $2\Theta = 14.8°$ to which no origin has been assigned. There is a small

TABLE III
Summary of Crystalline Melting Parameters for HPC/OSL Blends Prepared by Different Methods

Lignin content (wt %)	T_m (K)			ΔH_m (cal g^{-1})			$\Delta S_m \times 10^3$ (cal g^{-1} K^{-1})		
	Pyridine	Dioxane	Inj.-molded	Pyridine	Dioxane	Inj.-molded	Pyridine	Dioxane	Inj.-molded
0	484.8	483.0	484.6	1.07	1.01	1.01	2.21	2.09	2.08
5	481.6	480.7	480.6	0.99	0.72	0.72	2.06	1.50	1.50
10	473.9	475.4	474.2	0.88	0.65	0.58	1.86	1.37	1.22
15	468.6	469.0	468.6	0.85	0.57	0.54	1.81	1.22	1.15
20	463.1	462.4	463.3	0.73	0.47	0.49	1.58	1.02	1.06
30	453.1	458.3	453.1	0.61	0.35	0.42	1.35	0.76	0.93
40	444.3	453.0	443.9	0.30	0.29	0.31	0.68	0.64	0.70

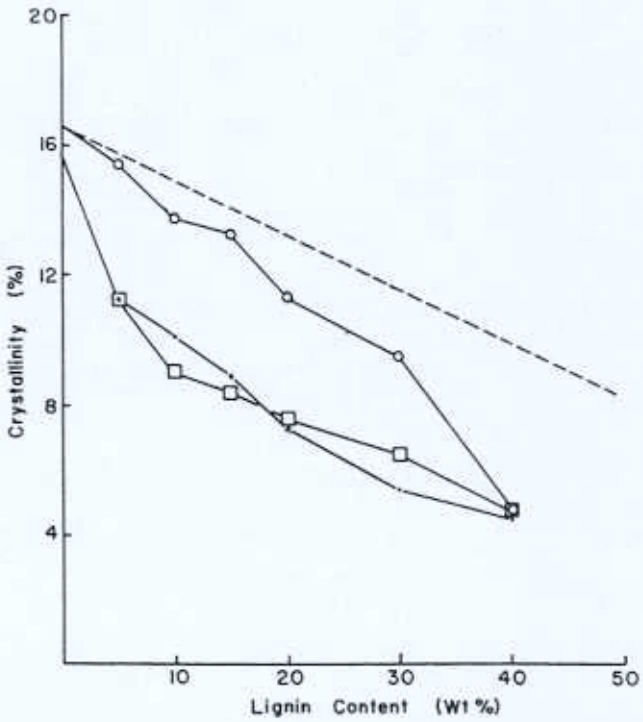

Fig. 4. The influence of blend composition on crystallinity for different preparation methods: (○) pyridine; (●) dioxane; (□) extruded.

increase in the position of the low angle peak as lignin content rises, and this returns to the original position with a small shoulder at 8.6°. This is of undetermined significance. Lignin content does not appear to affect the high angle peak.

Also presented in Figure 5 is the variation in the ratioed intensities of the two peaks (I-8°/I-20°) with blend composition. A consistent decrease in this ratio suggests an overall increase in the slightly oriented phase of the blend at the expense of crystalline structure. This result agrees with the observation by DSC of the degree of crystallinity (Fig. 4).

Experimental evidence by DSC and WAXS supports the presence of a crystalline HPC component in blends with lignin contents up to 40%. The T_g behavior then reflects the state of mixing in the amorphous phase; and, ideally, the melting point of the crystalline phase will be depressed by its equilibrium with the amorphous phase. The observed significant depression in T_m (ca. 40°, see Fig 4) allows an estimation of the intermolecular interaction parameter, B,[27] according to

$$\frac{-B}{RT_{m2}}\phi_1^2 = \frac{1}{T_{m2}} - \frac{1}{T_{m2}^0}\frac{\Delta H_{2u}}{RV_{2u}} + \frac{\ln \phi_2}{V_2} + \phi_1\frac{1}{V_2} - \frac{1}{V_1} \qquad (1)$$

where the subscript 2 refers to the crystallizable component (i.e., HPC), T_{m2}^0 is its equilibrium melting temperature, $\Delta H_{2u}/V_{2u}$ is its heat of fusion per unit volume of repeat unit for 100% crystalline material, V_2 is its molar volume,

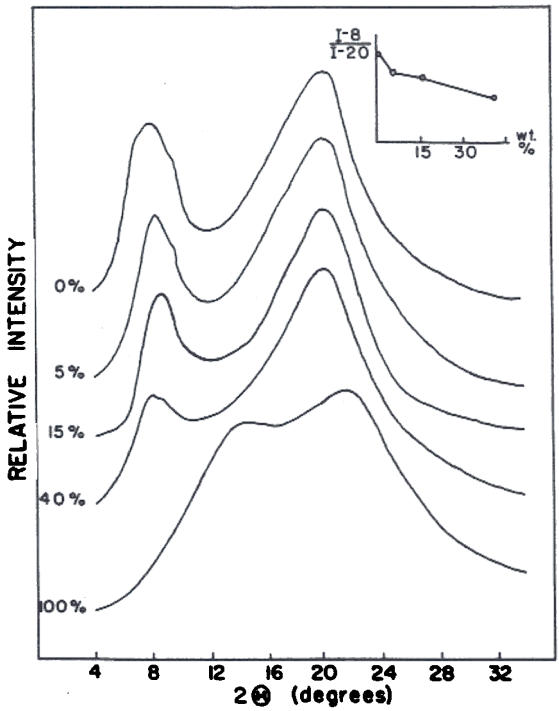

Fig. 5. Wide angle X-ray diffraction patterns for HPC/OSL blends cast from dioxane for lignin contents designated on the plot. Inset: Variation in the ratio of normalized peak intensities (I-8°/I-20°) with blend composition.

and ϕ_2 is its volume fraction in the blend. For blends with components whose molecular weight is > 2,000, V_1 and V_2 are large, and, (1) can be reduced to[28]

$$T_{m2}^0 - T_{m2} = \frac{-BV_{2u}}{\Delta H_{2u}} T_{m2}^0 \phi_1^2 \tag{2}$$

from which B can be directly evaluated from the slope of a plot of $(T_{m2}^0 - T_{m2})$ vs. ϕ_1^2. Figure 6 presents the results of this treatment with T_{m2}^0 of 486.2 K (213.1°C) as estimated by extrapolation to 0% lignin content. The value of $\Delta H_{2u}/V_{2u}$ has been reported previously[24] as 7.52 cal/cm^3, which leads to an estimated B value of -3.58 cal/cm^3 for the composite data. The negative B value provides additional support for miscibility between this polymer pair. While the observed behavior is adequately described by a linear model ($R^2 = 0.91$), the apparent curvilinear relationship which is observed may be an indicator of incipient phase separation. Also, no attempt was made to account for entropic contributions to T_m depression (e.g., a reduction in lamellar thickness of the crystallites), which are evident by the failure of the line to pass through the origin. Although some doubt may be cast on the magnitude of B, the negative value (suggesting secondary interactions) is not inconceivable considering the polarity of these two polymers. Further investigation into this aspect is warranted.

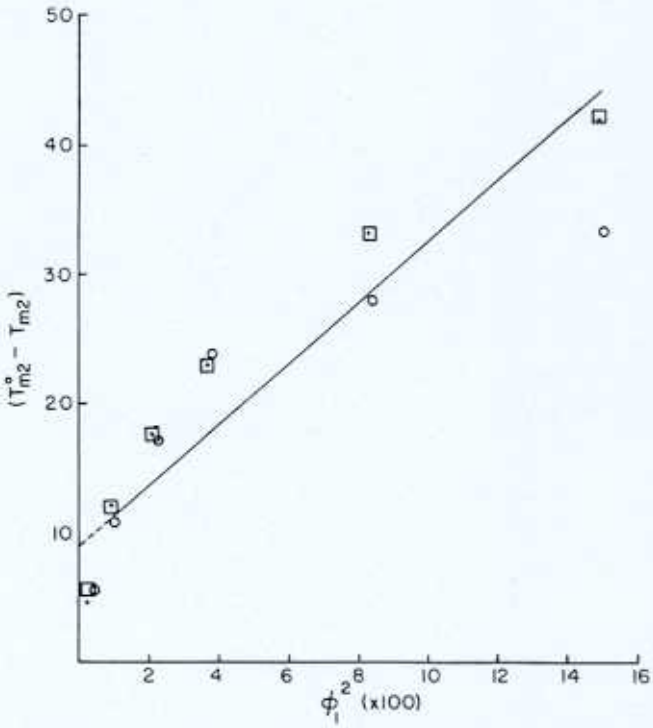

Fig. 6. Plot of $T_{m2}^{0} - T_{m2}$) vs. ϕ_1^2 for HPC/OSL blends prepared form dioxane (○), pyridine (●), and extrusion from the melt (□).

Fourier transform infrared spectroscopy (FTIR) has been used successfully in revealing specific interactions in miscible blends.[29] Small shifts in peak position are thereby interpreted with intermolecular interaction between polymer pairs. Application of this technique to the HPC/OSL blends failed to reveal changes indicative of interactions involving ether, carbonyl, or hydroxyl functionality. It must be concluded that the partial miscibility observered at low lignin content is best explained by the similarity of solubility parameters (i.e., 10.7[30] and 11.2[31] for HPC and lignin, respectively) rather than by polar–polar interaction between the component polymers.

Mechanical Properties

Results of stress–strain testing are presented in Figure 7. The injection-molded and dioxane-cast preparations are again distinguished from the blends prepared in pyridine. A dramatic increase in Young's modulus is observed in all blends, and this exceeds that predicted by the law of mixtures.[32] At 15% lignin content the modulus of the blends prepared in dioxane and by injection molding is ca. 50% higher than the predicted modulus. (Pyridine-cast blends exceed the prediction by ca. 25%.) The mechanical properties of these materials deteriorate at higher lignin contents. Tensile strength parallels modulus and presents an increase of 150% over the unmodified HPC at a lignin fraction of only 10% in the case of the molded blend while only moderate increases are found for the solvent cast series. A direct comparison between molded and

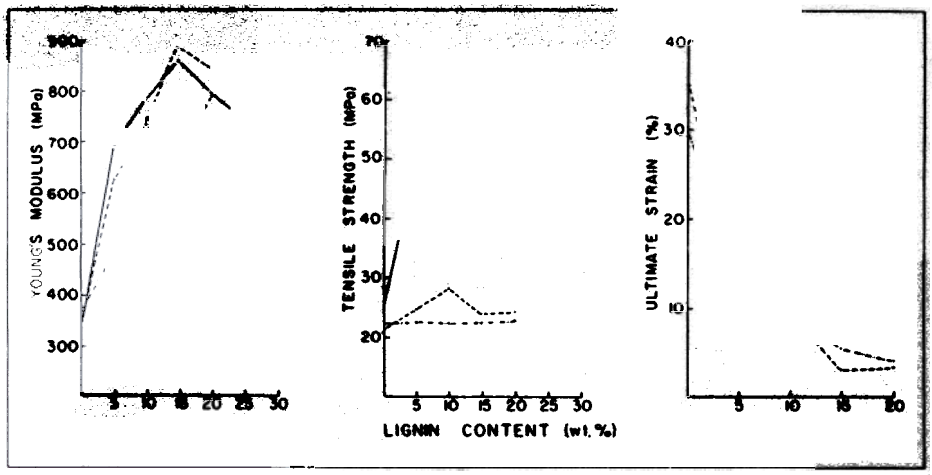

Fig. 7. The effect of preparation method and blend composition on the mechanical properties (Young's modulus, tensile strength, and ultimate strain) of HPC/OSL blends: (–·–·) pyridine-cast; (– – –) dioxane-cast; (——) melt extrusion.

solvent-cast blends may be tenuous since a significant difference in dimensions exists between these samples. The presence of microflaws in the material influences ultimate properties (but not modulus), and exerts a greater influence on the solvent-cast films which have a much smaller cross-sectional area than the injection-molded samples.

Ultimate strain levels achieved by the solvent-cast blends are also shown in Figure 7. (Extruded blends could not be determined because of grip failure.) Both blend types exhibit a rapid decline in ultimate strain from about 30 to 10%. This decrease in ultimate elongation accompanied by a rise in modulus and tensile strength (in the injection-molded blends) indicates orientation of HPC chains. Similar results on blends of a liquid crystal copolyester and amorphous polyamide were reported by Siegmann et al.[9] and compared to reinforced composites. This reinforcement is particularly unusual considering the low molecular weight of the lignin component (i.e., $M_n < 1{,}000$). The reinforcement may occur, however, from an elevated T_g due to compatibility of lignin with the amorphous HPC, resulting in the formation of a glassy matrix. As a result of the limited miscibility of the polymer pair, phase separation yields an LC mesophase structure, the organization of which may be assisted by the lignin molecules. By analogy, the resulting material exhibits behavior similar to that of a fiber-reinforced composite, particularly upon orientation of the LC component.

Blend Morphology

Scanning electron microscopy (SEM) was employed to further characterize the supermolecular morphology of the blends. Figure 8 shows the results of the freeze–fracture surface analysis for blends containing 15% lignin from all three preparation methods. Not surprisingly, the most dramatic difference is observed between the extruded and solvent-cast blends. A fibrous character is seen in the injection-molded samples, which is not observed in the unblended

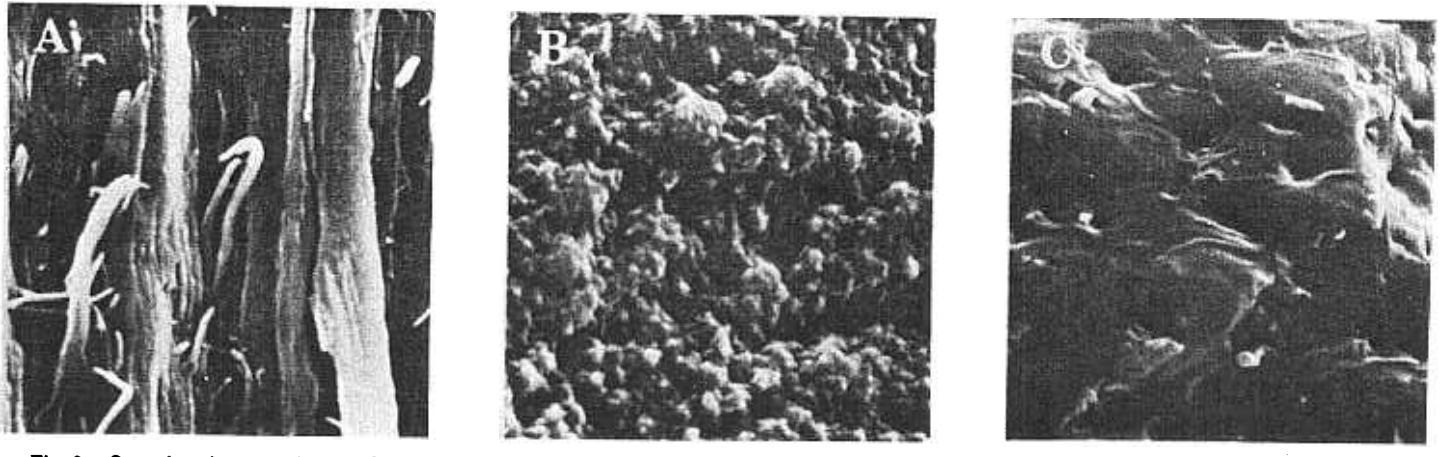

Fig. 8. Scanning electron micrographs of freeze-fracture surfaces of (A) extruded, (B) dioxane, and (C) pyridine blends at a composition of 15% lignin (magnification at 2,000×).

materials. This can be expected to account for the dramatic improvement in mechanical properties and implies orientation of the HPC chains as a result of lignin blending and melt extrusion. Interestingly, the utility of lignosulfonates in enhancing the fiber formation of low density polyethylene during extrusion has recently been reported.[33]

The differences between the two solution cast series are more subtle. A relatively smooth surface is seen with the pyridine sample which produced a sheetlike, or lamellar, fracture surface. By contrast, the dioxane-cast blend shows a rough surface, appearing nodular. Morphological studies of HPC have indicated that the basic supermolecular structural unit is a rounded particle resulting from the phase separation of liquid crystal structures during solvent removal.[26] The extent to which slippage and coalescence of these domains occurs during solvent evaporation (or induced orientation) largely determines specimen morphology. The molecular organization of the pyridine blend may not have advanced to the same degree as the dioxane blend. This remains, however, speculation, since the difference between the two solvent-cast blends is relatively obscure. Nevertheless, evidence from thermal and mechanical experiments indicates a certain degree of order in the HPC chains at low lignin contents. No evidence is seen for phase separation, at least in the classical sense, indicating miscibility of the polymer pair at lower (< 30%) lignin contents. This is consistent with observations made on the T_g behavior by DSC.

CONCLUSIONS

Blends of HPC and lignin represent a composite consisting of a pair of biopolymers in which one component is both a lyotropic and thermotropic liquid crystal polymer. This system holds promise for novel composite materials with an oriented liquid crystal component and high modulus and tensile strength.

Blends were prepared by casting from dioxane and pyridine solutions and by melting mixing and injection molding. Behavioral similarity was established between the dioxane-cast and molded preparations, rather than the two solution-blended series on the basis of the following findings:

1. A single T_g was observed for all preparations up to a composition of 40% lignin. The dioxane and molded blends exhibited positive deviation from additivity over this range while pyridine blends were well represented by this assumption.
2. Composition of the phases resulting from segregation at high lignin levels varied. The dioxane and molded blends exhibited signs of a phase with a T_g higher than that of the original components for lignin contents between 55 and 85%.
3. DMTA results suggested the presence of two relaxations in the temperature range between 25 and 125°C. These were attributed to an amorphous and a liguid crystal phase, respectively.
4. The melting and crystallization temperatures were not significantly influenced by the blending method, but exhibited a parallel, consistent decrease with rising lignin content.
5. The crystalline fraction of the blends decreased with lignin content.

6. The analysis of melting point depression yielded an intermolecular interaction parameter B of -3.58 cal/cm^3, suggesting strong secondary interactions between components.
7. No evidence of hydrogen bonding or other type of association was detected by FTIR.
8. Young's molulus increased by about 140% as lignin content rose to 15% in both dioxane-cast and molded materials. Although not as great, pyridine-cast blends also exhibited moduli well above that predicted by the rule of mixtures.
9. Tensile strength increased by about 150% when lignin content rose to 15% for injection-molded blends. Solution-cast blends were not as dramatically influenced.
10. Ultimate elongation decreased sharply, from about 30 to 5%, with the weight fraction of lignin rising to 15%.
11. The development of a fibrillar supermolecular morphology was evidenced by SEM for the molded preparations. Solution-cast blends did not reveal a given morphological feature.

The results allow the conclusion that the binary polymer pair represents a partially miscible system. The interaction between the two components is limited to the amophous phase of HPC, which comprises a lower volume fraction in the blends than in the pure component. A liquid crystal mesophase is formed when the casting solution reaches a critical concentration, or at appropriate temperatures. The ordered chains of the mesophase are dispersed in an amorphous matrix blend of lignin and HPC. The resultant material resembles a reinforced composite with enhanced mechanical properties.

The authors gratefully acknowledge the assistance of Dr. S. S. Kelley with the WAXS analysis and Mr. T. A. DeVilbiss with the FTIR analysis. Thanks also go to Hercules, Inc. for providing the hydroxypropyl cellulose. This study was financially supported by a grant from the National Science Foundation.

References

1. A. J. Yu, in *Multicomponent Polymer Systems*, Adv. Chem. Ser., No. 99. R. F. Gould, Ed., ASC Publications, Washington, D.C., 1971, p. 2.
2. S. L. Zacharius, W. J. MacKnight, and F. E. Karasz, in *Polymer Blends and Composites in Multiphase Systems*, Adv. Chem. Ser., No. 206. C. D. Han, Ed., ACS Publications, Washington, D.C., 1984, p. 17.
3. I. C. Sanchez, in *Polymer Blends*, Vol. 1. D. R. Paul and S. Newman, Eds., Academic Press, New York, 1978, Ch. 3.
4. T. Nishi and T. T. Wang, *Macromolecules*, **8**, 909 (1975).
5. D. C. Wahrmund, R. E. Berstein, J. W. Barlow, and D. R. Paul, *Polym. Eng. Sci.*, **18**, 683 (1978).
6. M. M. Coleman, J. Zarian, D. F. Varnell, and P. C. Painter, *J. Polym. Sci., Polym. Lett. Ed.*, **15**, 745 (1977).
7. W. J. Jackson and H. Kuhfuss, *J. Polym. Sci., Polym. Chem. Ed.*, **14**, 2043 (1976).
8. M. Takayanagi, T. Ogata, M. Morikawa, and T. J. Tai, *Macromol. Sci. Phys.*, **B17**, 591 (1980).
9. A. Siegmann, A. Dagan, and S. Kenig, *Polymer*, **26**, 1326 (1985).
10. E. G. Joseph, G. L. Wilkes, and D. G. Baird, in *Polymeric Liquid Crystals. Polymer Science and Technology*, Vol. 28, A. Blumstein, E., Plenum Press, New York, 1985, p. 197.
11. J. Watanabe, Y. Fukuda, R. Gehavi, and I. Uematsu, *Macromolecules*, **17**, 1004 (1984).

12. R. D. Gilbert and P. A. Patton, *Prog. Polym. Sci.*, **9**, 115 (1983).
13. E. Marsano, E. Bianchi, A. Ciferri, G. Ramis, and A. Tealdi, *Macromolecules*, **19**, 626 (1986).
14. E. Marsano, E. Bianchi, and A. Ciferri, *Macromolecules*, **17**, 2886 (1984).
15. K. Shimaura, J. L. White, And J. F. Fellers, *J. Appl. Polym. Sci.*, **26**, 2165 (1981).
16. S. Suto, M. Kudo, and M. Kararawa, *J. Appl. Polym. Sci.*, **31**, 1327 (1986).
17. D. A. I. Goring, in *Lignins: Occurrence, Formation, Structure and Reactions*, K. V. Sarkanen and C. H. Ludwig, Eds., Wiley-Interscience, New York, 1971, p. 748.
18. R. H. Atalla and U. P. Agarwal, *Science*, **227**, 636 (1985).
19. S. Sarkanen, D. C. Teller, J. Hall, and J. L. McCarthy, *Macromolecules*, **14**, 426 (1981).
20. T. K. Kwei, *J. Polym. Sci., Polym. Lett. Ed.*, **22**, 307 (1984).
21. J. R. Penacchia, E. M. Pearce, T. K. Kwei, B. J. Bulkin, and J.-P. Chen, *Macromolecules*, **19**, 973 (1986).
22. P. Luner and U. Kempf, *Tappi*, **53**, 2069 (1970).
23. D. R. Paul, J. W. Barlow, R. E. Berstein, and D. C. Wahrmund, *Polym. Eng. Sci.*, **18**, 1225 (1978).
24. R. J. Samuels, *J. Polym. Sci., A-2*, **7**, 1197 (1969).
25. D. G. Gray, *J. Appl. Polym. Sci., Appl. Polym. Symp.*, **37**, 179 (1983).
26. Y. Nishio and T. Takahashi, *J. Macromol. Sci., Phys.*, **B23**, 483 (1984).
27. P. J. Flory, *J. Chem. Phys.*, **17**, 223 (1949).
28. J. E. Harris, D. R. Paul, and J. W. Barlow, in *Polymer Blends and Composites in Multiphase Systems*, Adv. Chem. Ser., No. 206. C. D. Han, E., Am. Chem. Soc., Washington, D.C., 1984, p. 17.
29. M. M. Coleman and P. C. Painter, *Appl. Spectroscopy Rev.*, **20**, 255 (1984).
30. J. S. Aspler and D. G. Gray, *Polymer*, **23**, 43 (1982).
31. C. Schuerch, *J. Am. Chem. Soc.*, **74**, 5061 (1952).
32. R. P. Sheldon, *Composite Polymeric Materials*, Applied Science, New York, 1982, p. 76.
33. P. Albihn, B. Franzén, J. Kubát, and M. Rigdahl, *J. Appl. Polym. Sci.*, **32**, 4837 (1986).

Received January 5, 1988
Accepted February 19, 1988